

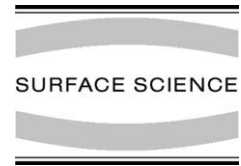


ELSEVIER

Available online at [www.sciencedirect.com](http://www.sciencedirect.com)

SCIENCE @ DIRECT®

Surface Science 538 (2003) L483–L487



[www.elsevier.com/locate/susc](http://www.elsevier.com/locate/susc)

Surface Science Letters

## Nanoridge domains in $\alpha$ -phase W films

J.P. Singh<sup>\*</sup>, T. Karabacak, T.-M. Lu, G.-C. Wang

*Department of Physics, Applied Physics and Astronomy, Rensselaer Polytechnic Institute, 110, 8th Street, Troy, NY 12180-3590, USA*

Received 9 April 2003; accepted for publication 12 May 2003

### Abstract

Two types of nanoridge domains oriented with each other with an angle ranging between  $109^\circ$  and  $124^\circ$  were measured by scanning tunneling microscopy on the  $\alpha$ -W film sputter deposited on an oxidized Si surface. Each domain contains nanoridges with a period of  $7.5 \pm 1.0$  nm. No such domains were observed on the  $\beta$ -W film surface. We argued that due to the anisotropy of the W(110) surface, the impinging W atoms diffuse faster along the  $\langle 111 \rangle$  directions on the surface to form the nanoridge structure. There are two equivalent  $\langle 111 \rangle$  directions, which give rise to two orientational domains with an angle of  $\sim 110^\circ$ . An isotropic  $\beta$ -W(100) phase has no preferred diffusion direction for the impinging W atoms and therefore, no nanoridge domain structure was observed.

© 2003 Elsevier B.V. All rights reserved.

**Keywords:** Scanning tunneling microscopy; Metallic films; Growth; Surface diffusion; Sputtering; Tungsten; X-ray scattering, diffraction, and reflection

Thin films of tungsten have been the subject of intense research due to their importance in a number of technological applications, for examples, diffusion barriers in semiconductor interconnect structures [1,2], absorbing layers in X-ray masks [3], and X-ray mirrors [4]. The physical, mechanical and optical properties of the film strongly depend on the film microstructure, which in turn is determined by the experimental conditions such as substrate temperature, substrate bias, deposition power, Ar gas pressure, and oxygen partial pressure in the chamber during the deposition process. Depending on the experimental

conditions, the resultant phase of the W film can be the  $\alpha$ -W, which has the equilibrium bcc structure, or the  $\beta$ -W, which has an A15 (cubic) structure, or a mixture of both phases [5–12]. It has been shown that the lattice parameter of the  $\beta$ -W phase monotonically decreases with increasing sputtering time until the  $\beta$ -W phase becomes unstable and turns into the  $\alpha$ -W phase [6]. Nanostructures, including a ridge-like structure, were reported on the stable  $\alpha$ -W films by atomic force microscopy [10]. The nature of these nanostructures is poorly understood. In this letter, we report a quantitative study of the nanoridge structure by using scanning tunneling microscopy (STM) and show that it contains two types of domains oriented to each other with a measured angle between  $109^\circ$  and  $124^\circ$ . We suggest that an anisotropic surface diffusion mechanism on crystalline W film

<sup>\*</sup> Corresponding author. Tel.: +1-51-8276-8387; fax: +1-51-8276-6680.

E-mail address: [singhj@rpi.edu](mailto:singhj@rpi.edu) (J.P. Singh).

is responsible for the formation of such nanostructures.

The tungsten films were deposited on polished p-Si(100) (resistivity 12–25  $\Omega$ cm) substrates in a dc planar magnetron sputtering system using a 99.95% pure W cathode. The vacuum chamber base pressure was  $1.4 \times 10^{-6}$  Torr during the film deposition. The p-Si(100) substrate was RCA cleaned [13] and mounted on a sample holder located at a distance of 15 cm from the cathode. After the RCA cleaning, the native oxide on the Si substrate was examined by reflection high-energy electron diffraction (RHEED). The diffraction pattern with only one specular spot confirms the amorphous nature of the top surface. In all the deposition experiments, the power was kept at 200 W and the Ar gas pressure was 1.5 mTorr. The maximum temperature of the substrate during the 65 min deposition was 80  $^{\circ}$ C. The thickness of a film was determined by measuring the step height between the masked and unmasked regions on the substrate using a stylus-type profilometer. The deposition rate was determined to be  $\sim 7$  nm/min. The X-ray diffraction (XRD) measurements were performed using a Scintag diffractometer with a Cu target operated at 50 kV and 30 mA to determine the  $\alpha$  and  $\beta$  phases. The diffractometer was calibrated with respect to the peak positions of a Si calibration standard. The surface morphology of W films was imaged by a homemade ultra high vacuum (UHV) STM system [14]. The tip used was made of Pt–Ir for its resistance against oxidation. All the STM measurements were performed in a vacuum chamber with a pressure better than  $5 \times 10^{-9}$  Torr. The images were obtained in a constant current mode with a set current of 1 nA and a bias voltage of 0.5 V applied to the W film surface.

The XRD spectra of W films are shown in Fig. 1. The thinner ( $\sim 70$  nm) film (Fig. 1(a)) was identified to have (200), (210), and (400) reflection peaks of a simple cubic A15  $\beta$ -W structure. The thicker ( $\sim 410$  nm) W film (Fig. 1(b)) was essentially a bcc  $\alpha$ -W structure with (110), (211) and (220) reflection peaks. The XRD spectrum of the bcc  $\alpha$ -W film showed a strong (110) preferred orientation. The lattice parameters calculated from the corresponding preferred orientations from the

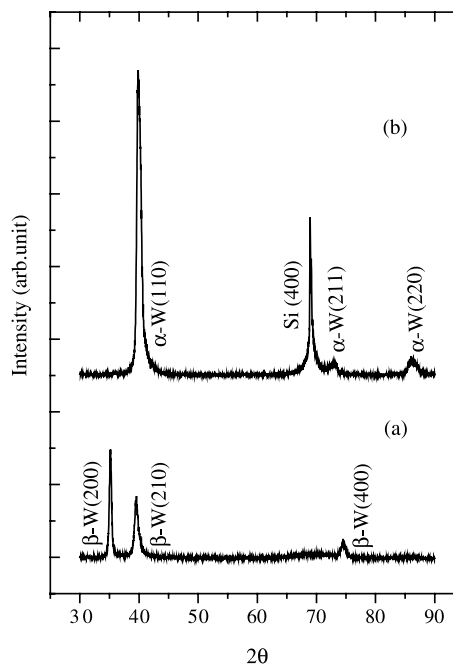


Fig. 1. The XRD spectra of (a)  $\sim 70$  nm and (b)  $\sim 410$  nm thick W films. The thinner film (a) shows the formation of the  $\beta$ -W phase, whereas the thicker film (b) shows the  $\alpha$ -W phase. A Si substrate peak is also observed in the thicker W film because the film was delaminating from the substrate due to the presence of large compressive stress.

XRD spectra are 0.30 nm for the bcc  $\alpha$ -W films and 0.49 nm for the A15  $\beta$ -W film, which are in good agreement with the reported bulk values of 0.31 and 0.50 nm, respectively [6].

The STM topographic images of the  $\alpha$ -W film surface are illustrated in Fig. 2. The surface is seen to have many grains and the grain boundaries were not well delineated (see Fig. 2(a)). A single grain having the nanoridge structure is shown in Fig. 2(b). The average grain size estimated from the STM images was  $130 \pm 15$  nm. More interestingly, many individual grains contain two types of nanoridge domains oriented with each other with an angle ( $\theta$ ) ranging between  $109^{\circ}$  and  $124^{\circ}$  as shown in Fig. 3(a). Each domain has ridges with an average height and period of  $1.5 \pm 0.5$  and  $7.5 \pm 1.0$  nm, respectively. These nanoridges were observed on the  $\alpha$ -W phase film surfaces irrespective of the film thickness. No such structure was observed on the  $\beta$ -W film surface (Fig. 3(b)). The

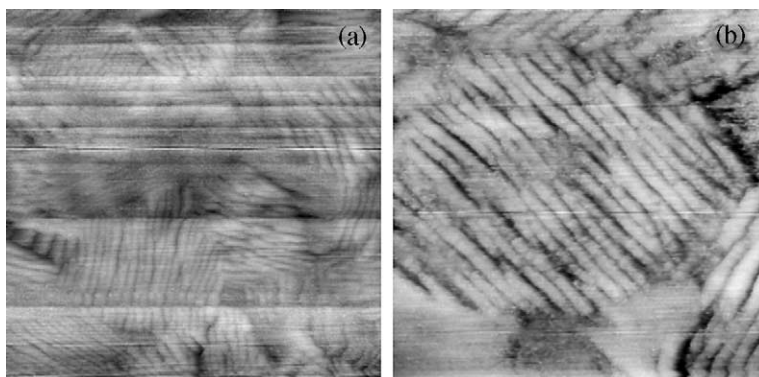


Fig. 2. (a)  $400 \times 400 \text{ nm}^2$  and (b)  $200 \times 200 \text{ nm}^2$  STM images of  $\sim 410 \text{ nm}$  thick  $\alpha\text{-W}$  film surface. A single grain having the nanoridge structures is seen in (b).

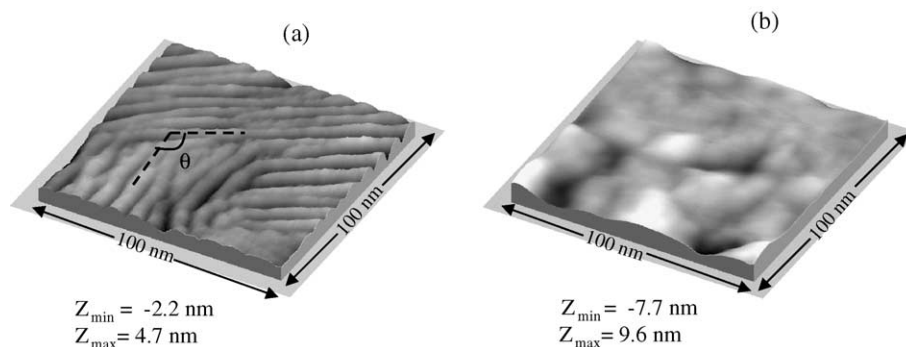
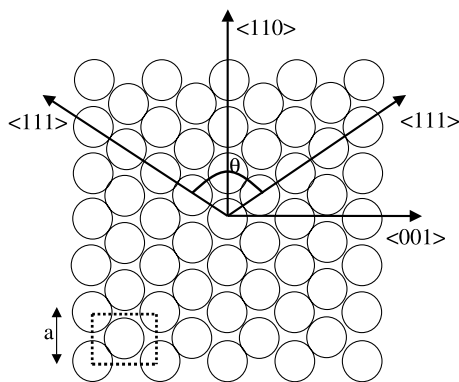


Fig. 3. The  $100 \times 100 \text{ nm}^2$  STM images of (a)  $\sim 410 \text{ nm}$  thick  $\alpha\text{-W}$  and (b)  $\sim 70 \text{ nm}$  thick  $\beta\text{-W}$  films. The  $\alpha\text{-W}$  film surface shows the formation of two types of nanoridge domains oriented with each other by an angle ( $\theta$ ) that lies between  $109^\circ$  and  $124^\circ$ . The  $\beta\text{-W}$  film surface appears to have smooth grains with no ridge structures.

XRD results in Fig. 1 suggest that initially the film grows in the  $\beta\text{-W}$  phase and eventually transforms into the  $\alpha\text{-W}(110)$  phase. This is consistent with the results reported by previous researchers that the  $\beta\text{-W}$  phase undergoes a structural transition to the  $\alpha\text{-W}$  phase with increasing sputtering time or the thickness of the film [2,6]. In this regard, Weerasekera et al. [6] have observed the decrease in the oxygen partial pressure due to the gettering of oxygen impurity into the freshly formed W film, which leads to the  $\beta\text{-}$  to  $\alpha\text{-W}$  phase transition for longer sputtering times.

The surface lattice structures of the  $\alpha\text{-W}(110)$  plane is shown in Fig. 4. Every atom in the topmost layer has four nearest-neighbors and two next-nearest-neighbors located at the distances of  $\sqrt{3}a/2$  and  $a$  in the topmost layer, respectively,

where  $a$  is the lattice constant of bcc  $\alpha\text{-W}(110)$  structure. The  $\langle 111 \rangle$  directions (see Fig. 4) are inclined at  $\sim 110^\circ$  to each other. The anisotropy in diffusion barriers along different directions is large and therefore W adatom motion on the  $\text{W}(110)$  plane should differ in different directions. Ehrlich and Hudda [15] have done a detailed study of the self-diffusion of W on W lattice by using field ion microscopy (FIM). It was shown that the surface diffusion not only depends on the plane index but also on the crystallographic directions on a particular plane and can be anisotropic. Because of this anisotropy, formation of one dimensional chain structures and fractals on the surface were reported in the literature [16–18]. For example, the anisotropy in surface diffusion was observed for the Cu growth on the  $\text{W}(110)$  plane [18]. The



W (110) plane

Fig. 4. A schematic diagram of W(110) surface lattice structure showing the crystallographic directions. A rectangular primitive cell is also shown. The  $\alpha$ -W(110) has a lattice constant of 0.316 nm and the angle  $\theta$  between the  $\langle 111 \rangle$  directions is  $\sim 110^\circ$ .

activation energy for diffusion  $E_s$  depends on the jump direction. The  $E_s$  is equal to 0.3 eV for jumps in the  $\langle 111 \rangle$  direction and the  $E_s$  equal to 0.85 eV for jumps in the  $\langle 100 \rangle$  direction [18].

In the sputter deposition once the  $\alpha$ -W phase is initiated the sputtered W atoms impinge upon the W(110) lattice have a preferred surface diffusion along non-orthogonal  $\langle 111 \rangle$  directions, the channels of high mobility, i.e. low potential barriers. Turner et al. [19] have shown from their Monte Carlo simulations that the impact energy of W atoms can be as high as  $\sim 20$  eV at 2 mTorr Ar gas pressure. Therefore, the sputtered W atoms have sufficient energies to overcome the surface diffusion potential barriers along different directions on the W(110) plane but will have an orientation effect towards the high mobility  $\langle 111 \rangle$  channels. Since tungsten has a very high melting temperature ( $T_M = 3683$  K), the structures once created during the film growth will be frozen in after the film deposition. This leads to the formation of nearly parallel nanoridges over the  $\alpha$ -W(110) film surface as observed in the STM images in Fig. 3. The nanoridges were formed along the two  $\langle 111 \rangle$  directions oriented by an angle of  $\sim 110^\circ$  with each other, which leads to the formation of two types of nanoridge domains on the  $\alpha$ -W film surface. In a recent study, Oh et al. [20] have shown that al-

though the self diffusion of W on W(110) plane is mainly along the  $\langle 111 \rangle$  directions, the jumps along  $\langle 001 \rangle$  and  $\langle 110 \rangle$  are still important and can give significant atomic displacements. This may cause the widening of the nanoridge structures.

The  $\beta$ -W is not an amorphous phase but a disordered A15 cubic phase that consists of simple cubic unit cells [5,7,11]. Therefore, there is no preferred direction for diffusion of the impinging sputtered W adatoms on the  $\beta$ -W film surface. Thus, no ridge patterns were visible on the  $\beta$ -W film surface (see Fig. 3(b)). Instead, the surface topography shows the smooth and fine grain structure. All the W film depositions were performed on the native oxide of the Si substrate that is amorphous in nature. Therefore, the formation of nanoridge structures due to an ordered substrate is ruled out. In the literature [8], these nanoridge structures were not observed on very thin W films ( $\sim 10$  nm) grown on  $\text{SiO}_2$  by the electron beam evaporation. This shows that the formation of nanoridges is a result of the growth of W on a crystalline W(110) and not a result of the nucleation of W on  $\text{SiO}_2$  substrate.

In summary, the STM topography images on W films show the formation of two types of nearly parallel nanoridge domains oriented with each other on the  $\alpha$ -W surface by an angle ranging between  $109^\circ$  and  $124^\circ$ , whereas no such patterns were visible on the  $\beta$ -W film surface. We interpret that the anisotropic surface diffusion of sputtered W particles over the  $\alpha$ -W(110) surface leads to the formation of nanoridge domains oriented in the high mobility  $\langle 111 \rangle$  directions. Whereas, an isotropic  $\beta$ -W phase has no preferred diffusion direction for the impinging sputtered W particles and therefore, no nanoridge pattern was observed.

### Acknowledgement

The work was supported by NSF DMR.

### References

- [1] K.Y. Ahn, Thin Solid Films 153 (1987) 469.
- [2] S.M. Rosnagel, I.C. Noyan, C. Cabral Jr., J. Vac. Sci. Technol. B 20 (2002) 2047.

- [3] M. Itoh, M. Hori, S. Nadahara, *J. Vac. Sci. Technol. B* 9 (1991) 149.
- [4] M.S. Aouadi, R.R. Parsons, P.C. Wong, K.A.R. Mitchell, *J. Vac. Sci. Technol. A* 10 (1992) 273.
- [5] Y.G. Shen, Y.M. Mai, *Mater. Sci. Eng. A* 284 (2000) 176.
- [6] I.A. Weerasekera, S.I. Shah, D.V. Baxter, K.M. Unruh, *Appl. Phys. Lett.* 64 (1994) 3231.
- [7] M.J. O'Keefe, J.T. Grant, *J. Appl. Phys.* 79 (1996) 9134.
- [8] R.S. Wagner, A.K. Sinha, T.T. Sheng, H.J. Levinstein, F.B. Alexander, *J. Vac. Sci. Technol.* 11 (1974) 582.
- [9] M. Haghiri-Gosnet, F.R. Ladan, C. Mayeux, H. Launois, M.C. Joncour, *J. Vac. Sci. Technol. A* 7 (1989) 2663.
- [10] K.L. Westra, D.J. Thomson, *Thin Solid Films* 257 (1995) 15.
- [11] Y.G. Shen, Y.W. Mai, Q.C. Zhang, D.R. McKenzie, W.D. McFall, W.E. McBride, *J. Appl. Phys.* 87 (2000) 177.
- [12] C.M. Falco, *J. Appl. Phys.* 56 (1984) 1218.
- [13] W.A. Kern, *RCA Rev.* 31 (1970) 207.
- [14] A. Chan, *Scanning tunneling microscopy: construction and its application to study of rough surfaces* Ph.D. thesis 1996, Rensselaer Polytechnic Institute, Troy, NY.
- [15] G. Ehrlich, F.G. Hudda, *J. Chem. Phys.* 44 (1966) 1039.
- [16] H. Brune, *Surf. Sci. Rep.* 31 (1998) 121.
- [17] K. Hara, K. Itoh, M. Kamiya, H. Fujiwara, K. Okamoto, T. Hashimoto, *Jpn. J. Appl. Phys.* 33 (1994) 3448.
- [18] J.M. Rogowska, M. Maciejewski, *Vacuum* 63 (2001) 91.
- [19] G.M. Turner, I.S. Falconer, B.W. James, D.R. McKenzie, *J. Vac. Sci. Technol. A* 10 (1992) 455.
- [20] S. Oh, K. Kyuno, S.J. Koh, G. Ehrlich, *Phys. Rev. B* 66 (2002) 233406.